Weld Stresses Beyond Elastic Limit

Materials Discontinuity

V. Verderaime
George C. Marshall Space Flight Center
Marshall Space Flight Center, Alabama

ACKNOWLEDGMENTS

TABLE OF CONTENTS

PRECEDING PAGE BLANK NOT FILMED

LIST OF ILLUSTRATIONS

THIS DOCUMENT PROVIDED BY THE ABBOTT AEROSPACE
TECHNICAL LIBRARY
ABBOTTAEROSPACE.COM

TECHNICAL PAPER

WELD STRESSES BEYOND ELASTIC LIMIT
1. Material Discontinuity

I. INTRODUCTION

Many spacecraft structures are required to be verified with a minimum safety factor of 1.1 on yield and 1.4 on ultimate strength [1] which, in the design phase, are both conservatively complied with in a linear fashion [2]. As the structure progresses through the operational phase and prevailing environments begin to exceed original design requirements, safety demands that current margins be affirmed. Determination of post-development safety factors on yield are linear and are usually accommodated, but ultimate strength predictions involve nonlinear considerations not commonly understood. The intent of this paper, the first in a series of three reports, is to provide mechanics insights to questions raised by Dr. George McDonough [3] on aluminum welded joint behavior beyond the elastic limit.

The modified aft skirt structure of the solid rocket booster (SRB) was analyzed to predict safety margins using updated launch pad loads. Detailed global and substructural models were developed using a finite element method (FEM). The critical area was identified to be the aluminum weld joining the shell and a holddown post forging, because the weld material had a lower yield point and ultimate strength than adjacent parent metals. The weld was modeled with brick elements, five across the width, and the FEM code iterated the inelastic material properties in a piece-wise-linear routine [4]. While the model predicted positive margins on the ultimate, the structural test article failed at the weld interface 8 percent below the required safety factor and at half the expected elongation. Twenty-four weld specimens were cut from the remaining skirt structure and uniaxially tested. All specimens were noted to fail at weld-parent interfaces. Average tensile design properties were reported and are included in Appendix A.

Significant questions raised by this experience were:

1. What does consistent weld fracture at the interface imply?

2. What is the effect of relative property differences between weld and parent materials on interface fracture?

3. Is there a mechanics relationship between geometry and strength?

4. What insights and considerations might be extended to FEM modeling?

5. How much reliability was lost by the negative margin in post-development analysis?

Of course there are many more questions, but these are vital for the revisit to the aft skirt design and for the choice of fabrication technology of future high performance structures. All of them have been addressed in some fashion in the past. Certainly, metallurgists have grappled extensively with the interface problem for years and are currently investigating it for the skirt failure. This paper responds to

the first four questions in some depth from a mechanics viewpoint and spills into a discussion on the last question. The most difficult task in relating the unknown interface phenomenon to a conceived model was not to find an elegant, or even an exact, approach, but to find any method at all that might describe the suggested physics.

II. WELD INTERFACE STRESSES

Perhaps the first suggestion that a discontinuity stress was acting at the weld interface came from Mr. Timothy P. Vaughn's strain gage data [5] based on a uniaxial test of weld specimen (see Figure A-1 in Appendix A). At 45-ksi stress, the gage on the weld center was indicating 0.022 strain, while gages at the plate and forging interfaces were reading about 4 percent higher strains. Parent plate strain away from the weld was less than 0.01. Metallurgical faults influencing consistent boundary fracture not excluded, it was thought that increased strain at both boundaries and fracture might be partially explained through mechanics.

Referring to the stress-strain data (see Figure A-2 in Appendix A), at 45-ksi stress the plate is slightly strain hardened and the weld is far into it. The Poisson's ratio for the plate is just a bit higher than elastic, but the weld is approaching 0.5. Consequently, under uniaxial tensile stress, lateral strains and related displacements at the interfaces should be sufficiently different to cause local discontinuity stresses.

The approach was to model the test specimen, predict stresses and strains for the plate-weld boundary, and compare results with test gage data. Since discontinuity peak stresses dissipate over a very small span, a classical elasticity model was believed to define it more sharply than the FEM. Furthermore, simplified assumptions could be more easily tracked and results intuitively qualified accordingly. The discontinuity model contrived is presented in Appendix B. It satisfies interface boundaries, and stress distributions are developed independently of material properties. Nonlinear properties required to determine displacements and strains are applied piece-wise linear.

1. Uniaxial Specimen Stresses

As a uniaxial tensile stress, σ_x, is applied to the test specimen, the half thickness "h" contracts laterally a quantity v_p along the plate and a greater quantity v_w along the weld because of differences in Poisson's ratio beyond the elastic limit (Fig. 1).

This difference in lateral contraction may be expressed by

$$\Delta v = \sigma_x h K \frac{\mu}{E} \quad , \tag{1}$$

where K is a simplified but effective relative material index defined by

2

$$K = \left[\frac{\mu_p}{E_p} - \frac{\mu}{E} \right] \frac{E}{\mu} \quad . \tag{2}$$

It varies between 0 and -1, and resembles Figure 1 more as it approaches -1. Plate materials are referenced by a subscript (p) and weld properties are not subscripted. Moduli and Poisson's ratios are calculated from Appendix A.
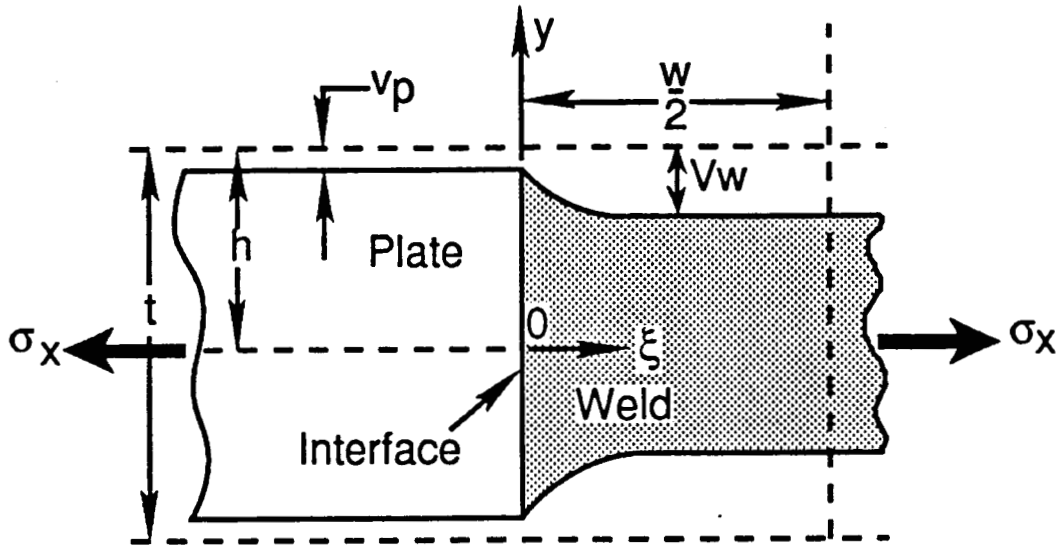

Figure 1. Lateral contraction under uniaxial stress.

At the interface, $\xi = 0$, the differential displacement of plate and weld must match according to

$$\Delta v(\sigma_x) + v(q) = 0 \quad , \tag{3}$$

where the first term is the relative displacement caused by the applied axial stress, σ_x, as determined from equation (1). The second term is the local stretching required from a dummy unit loading, q, acting adjacent to the interface to conform to the displacement of the first term. This second term was derived using stress-strain relationships, and discontinuity factors D_y and D_x were developed in Appendix B to give

$$\frac{v(q)}{q} = \frac{\varepsilon_y h}{q} = \frac{h}{E} [D_y - \mu D_x] \quad . \tag{4}$$

Substituting equations (B-7), (1), and (4) into (3) gives the desired ratio of applied axial stress to applied dummy loading,

3

$$D_{\sigma.q} = \frac{\sigma_x}{q} = -\frac{2}{\mu K}\left[T + (1-\mu)\sum \frac{1}{\alpha} \sin(2T\alpha)\right] . \tag{5}$$

Equation (5) is corrected for Gibb's phenomenon at the interface x = d and is expressed in parametric form. Convenient parametric identities are

$$T = \frac{d}{L}, \quad H = \frac{h}{L}, \quad X = \frac{x}{L}, \quad Y = \frac{y}{L}, \quad \text{and} \quad \alpha = m\Pi . \tag{6}$$

Using identities (6) into equation (B-7), stress discontinuity factors in the weld region are expressed in the following parametric form:

$$D_{xy} = 4\sum \sin(\alpha T) \sin(\alpha X) [H \sinh(\alpha Y) - Y \cosh(\alpha Y)] e^{-\alpha H}$$

$$D_y = T + 4\sum \sin(\alpha T) \cos(\alpha X) \left[\left(H + \frac{1}{\alpha}\right)\cosh(\alpha Y) - Y \sinh(\alpha Y)\right] e^{-\alpha H}$$

$$D_x = 4\sum \sin(\alpha T) \cos(\alpha X) \left[Y \sinh(\alpha Y) - \left(H - \frac{1}{\alpha}\right)\cosh(\alpha Y)\right] e^{-\alpha H} . \tag{7}$$

In applying these equations, note the two coordinate systems between Figures 1 and A-1. When $\xi = 0$, x = d, and when $\xi = w/2$, x = L.

Finally, net distribution factors of stress components acting in the weld are related to the applied axial stress by dividing equation (7) by (5) and superimposing the applied stress to the axial equation:

$$S_{xy} = \frac{\tau_{xy}^d}{\sigma_x} = \frac{D_{xy}}{D_{\sigma.q}} ; \quad S_y = \frac{\sigma_y^d}{\sigma_x} = \frac{D_y}{D_{\sigma.q}} ; \quad S_x = \frac{\sigma_x^d}{\sigma_x} = 1 + \frac{D_x}{D_{\sigma.q}} . \tag{8}$$

Superscript d denotes that discontinuity stresses are included and σ_x is the applied axial stress, as defined before. Using equation (8) and properties of weld test specimen at 45-ksi applied stress,

	Plate	Weld	
ε	0.014	0.024	K = -0.49
μ	0.40	0.46	T = 0.2
E	3135	1840	H = 4.6 ,

$$\tag{9}$$

4

the computed distribution factors of stress components of equation (8) are graphically presented in Figure 2.

Though these results cannot be adequately verified, there were two gage data points on the specimen surface that were thought to be correlatable; the weld midwidth strain gage and the interface gage which read 4 percent higher than the midwidth. Surface axial stress factor (S_x) predictions of equation (8) were obtained from the bottom chart of Figure 2 for $y/h = 1.0$. The two test strain gage locations were $\xi/w = 0$ and 0.5 corresponding to an interface estimated stress factor of 1.07 and midweld of 0.96.
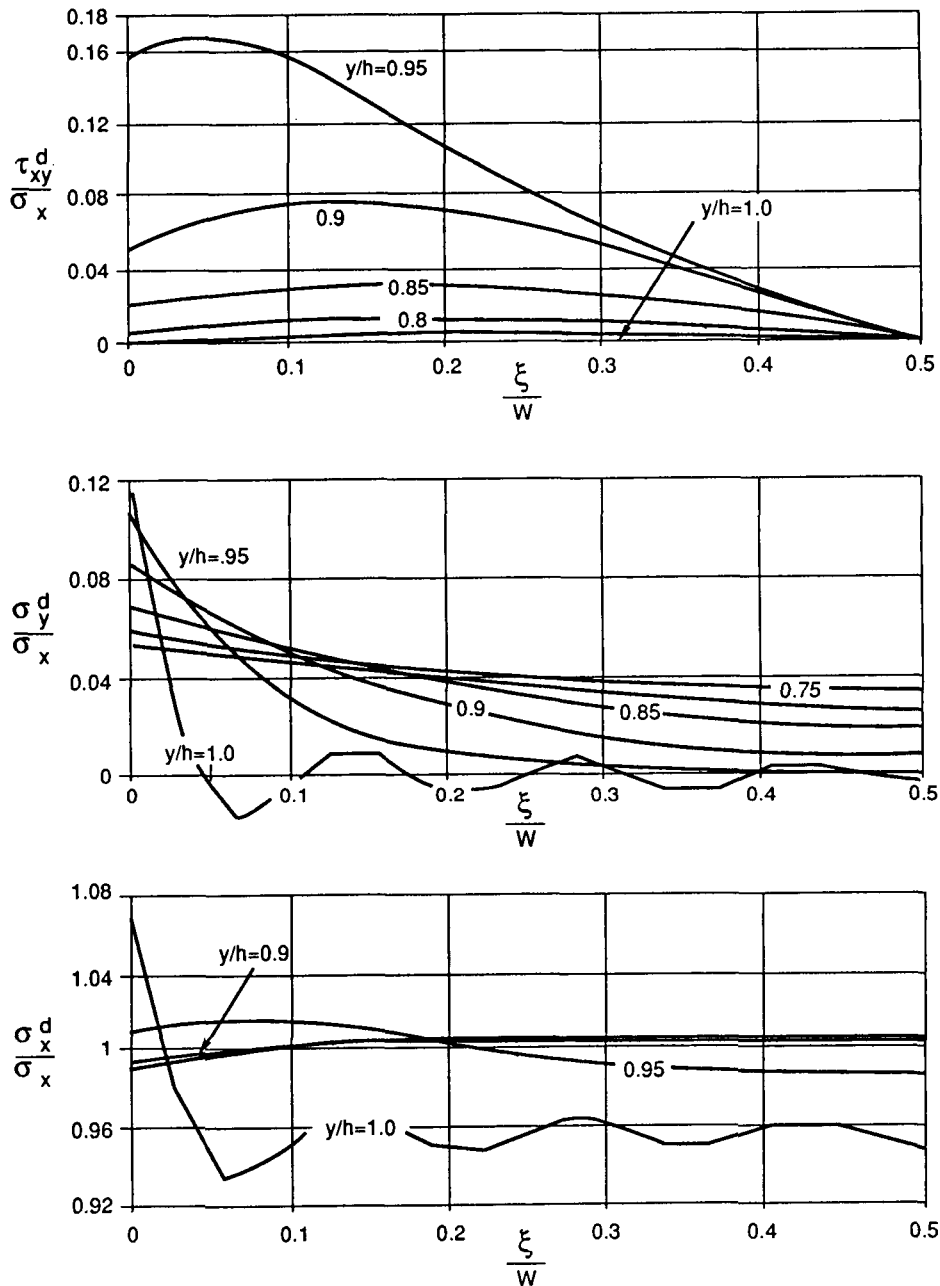

Figure 2. Discontinuity factors of stress components in uniaxial specimen.

It was interesting to note that the midweld stress predicted at the surface was 4 percent less than the applied axial stress while subsurface stresses were equal to the applied stress. The net outcome was that the interface stress on the surface was a net 11 percent higher than at the weld midwidth. Referring to equation (A-3), an 11 percent variation of stress on the weld material translates to

$$\delta\varepsilon = \frac{1}{0.23}\, \delta(11) = 48\% \text{ strain} \tag{10}$$

increase at the interface. However, this strain was acting over a very narrow band of $\Delta\xi/w = 0.05$, which was approximately 0.016 inches. The strain gage length was 0.125 inches which spanned over a weld strain of 0.024, and an interface strain of 0.036. Since changes in strain gage resistance in the two regions were in series, the interface strain gage net prediction was determined from the rule of mixtures to be 0.025, which was 4.5 percent higher than the midwidth location.

This correlation was not entirely conclusive because it depended on dubious strain gage locations. If the gage span included a portion of the plate, the gage pickup would be less. If the plate material at the interface was softened by the welding heat, the gage reading would be higher, but the discontinuity factor would be less. The only point made clear so far was that, if an abrupt change of metallurgical properties occurs at the weld interface, then a stress riser could be induced and its characteristics would be consistent from weld to weld. This point was pursued further for other mitigating implications.

2. Interface Discontinuity Stress Assessment

If discontinuity stresses are inherent at weld interfaces, then welds should consistently fail at interfaces with predictable strength, and uniaxial tension test data should reflect the design property of this weakest link. Beyond that, designers must also know how discontinuity stress factors vary with other weld parameters. There is a need to know (1) how distortion energy theory of failure of combined stresses at the interface compares with the surface axial stress, and (2) how sensitive is the stress factor to material pairing using some relative material index.

Distortion energy stresses are similarly derived in parametric form from the combined stress components of equation (8). Starting with the stress tensor,

$$\begin{vmatrix} (S_x - \lambda) & S_{xy} \\ S_{xy} & (S_y - \lambda) \end{vmatrix} = 0 \quad ,$$

principal stress factors are determined,

$$S_{1,2} = \frac{S_x + S_y}{2} \pm \frac{1}{2}[(S_x + S_y)^2 - 4(S_x S_y - S_{xy}^2)]^{0.5} \quad . \tag{11}$$

6

These principal factors are substituted into the distortion energy theory,

$$S_0^2 = S_1^2 + S_2^2 - S_1 S_2 \quad ,$$

so that

$$S_0 = [S_x^2 + S_y^2 - S_1 S_2 + 3 S_{xy}^2]^{0.5} \quad . \tag{12}$$

The theory hypothesizes that a material will fail when the energy of distortion of combined stresses achieves the same energy for failure in simple tension.

The distortion energy stress factor distribution over the weld is plotted in Figure 3. Again, as for the discontinuity factor in Figure 2, the surface energy factor away from the interface is less than the applied axial stress. This implies that test stress-strain relations based on surface strains are not conservative. Those below the surface are reasonably close to the applied stress, as they should be, to comply with the distortion energy theory. The peak value occurs on the surface at the interface, which is only 1.5 percent higher than the applied stress.
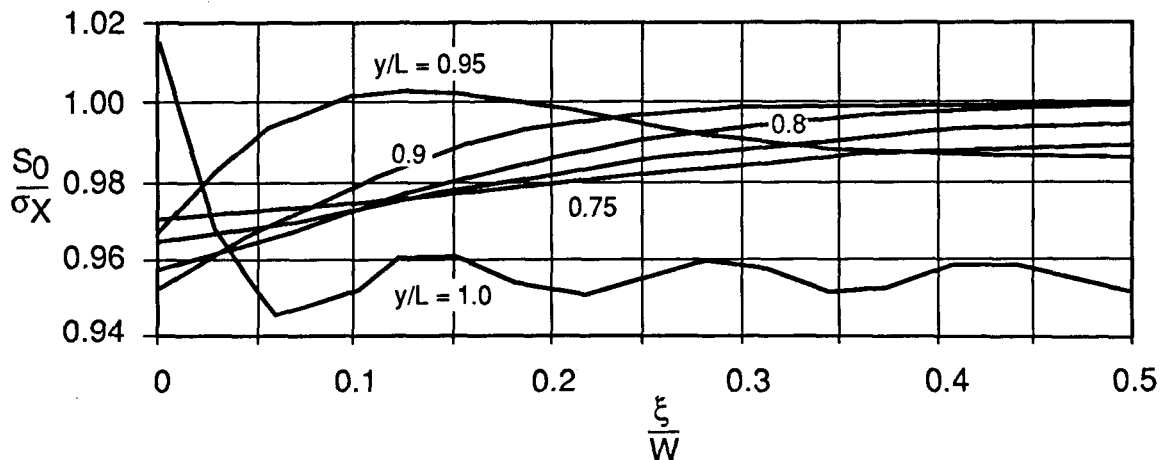

Figure 3. Distortion energy stress factor.

Actually, distortion failure factors should be calculated at the failed applied stress of 49 ksi. Equation (1) shows the relative displacement between plate and weld to be directly proportional to the material property K. Since discontinuity stress factors are also directly related, they should increase with increase in K, as noted in Figure 4. The recalculated properties at weld failure of 49 ksi, index $K = -0.5$, and $\mu = 0.5$, produced an energy failure factor of $S_0 = 1.03$ and a strain increase of 1 percent. Even for the worst case pairing of materials, the distortion failure stress factor at the interface of a uniaxial specimen is not very sensitive to materials.
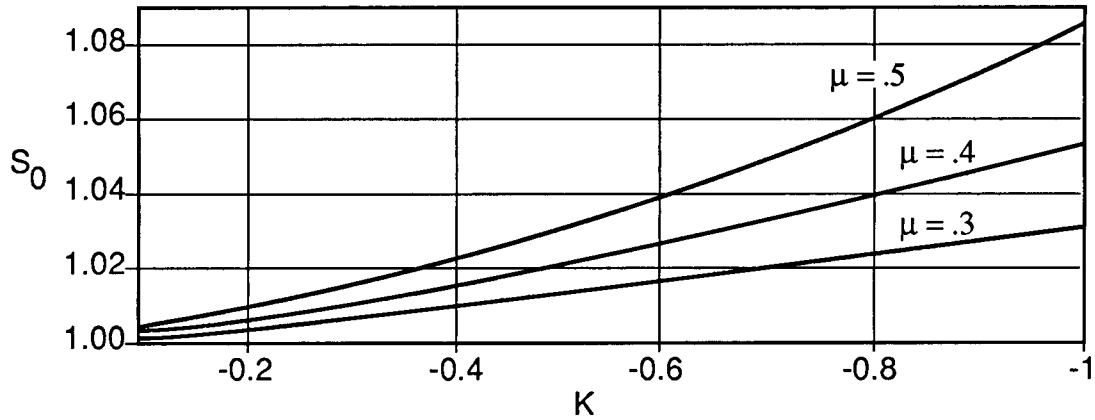
Figure 4. Material properties effects on uniaxial failure factor.

3. Discontinuity Stresses in Plane Strain

Consider a specimen having a very large width such as to ensure plane strain condition. How does the distortion failure factor vary in a different stress field? The only required modifications to the analysis are the relative material index,

$$K_b = \left[(1 + \mu_p) \frac{\mu_p}{E_p} - (1 + \mu) \frac{\mu}{E} \right] \frac{E}{(1 + \mu)\mu} \quad , \tag{13}$$

and the ratio of applied axial-to-dummy stresses,

$$D_{\sigma,q} = \frac{\sigma_x}{q} = -\frac{2}{\mu K_b} \left[T(1 - \mu) + (1 - 2\mu) \sum \frac{1}{\alpha} \sin(2T\alpha) \right] \quad . \tag{14}$$

Incorporating these revised expressions to the above equations, the results are shown in Figure 5. Obviously, externally-imposed biaxial stress conditions have a decisive effect on the failure factor as it approaches ultimate stress and $\mu = 0.5$. This is a particularly meaningful discovery because the SRB aft skirt weld is in a biaxial stress field and the allowable weld strength was based on uniaxial test data. Consequently, the skirt failure is expected to always occur at the weld interface and at a lower strength than current predictions; perhaps 10 percent.
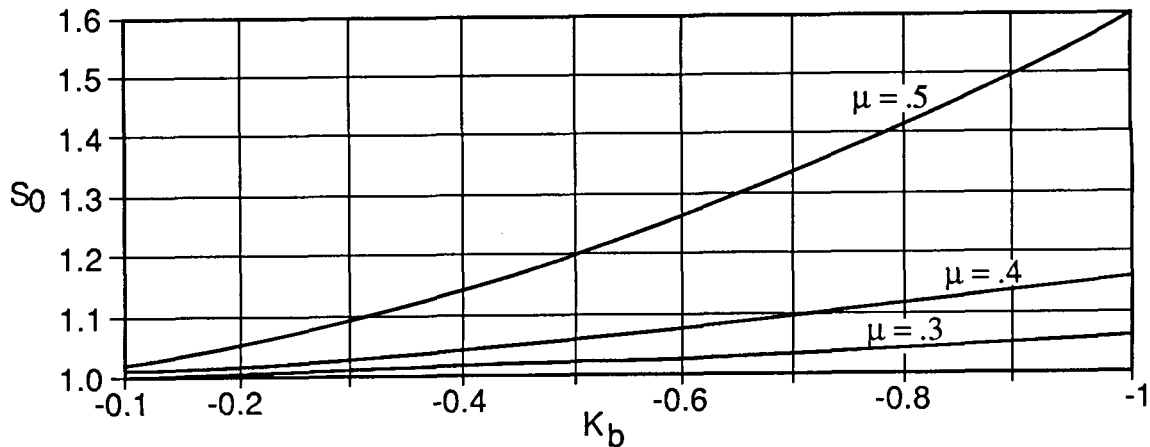
8

Figure 5. Plane strain effects on distortion failure factor.

4. Implications to Other Fracture Issues

There are four types of discontinuity stresses caused by abrupt changes in materials, geometry, loads, and temperature. Each may be solved piece-wise linear in the inelastic range, but whether any combination of the four occurring simultaneously may be linearly added needs to be established in fact. The aft skirt welds had three types of discontinuities at the holddown post fillet which compounded the failure predictability.

If the same ultimate factor of safety is to be imposed on structures during development and post-operations, then more exploratory-type test programs in the inelastic range are required to provide appropriate design data and to verify nonlinear math models and prediction techniques.

There are many conditions and opportunities for introducing metallurgical defects and distortions in aluminum weld interfaces [6] and particularly in large structures. Fortuitously, the weld peak failure stress occurs on the surface at the interface which can be inspected for flaws and other contributing deficiencies. However, weld discontinuity stresses do not seem to present a risk to fracture mechanics because the bandwidth of the peak stress field at the interface is much narrower than a practical flaw size. On the other hand, if the discontinuity failure factor is large, the fatigue life is reduced accordingly.

III. SUMMARY

When stress-strain relationships between weld and parent materials are appreciably different, discontinuity stresses at interfaces might be considered. If the weld consistently fails at the interface with no obvious metallurgical defect, then discontinuity stresses are a strong suspect. There are no straight-forward tests to detect them, but mathematical predictions followed by tests might provide implicit results and foundation to resolve this intriguing phenomenon.

The analysis presented and possible FEM techniques have their limitations. As stated before, the purpose for selecting the classical mechanics model was so discontinuity values and bandwidths might be more sharply defined. Perhaps iterating on nonlinear material properties might have improved resulting stress factors, but the motive for this analysis was to learn if there was a mechanics problem in the first place, and then to obtain insights on its implication in other related issues.

Nevertheless, it may be concluded that 2219 aluminum weld material is sufficiently dissimilar from the parent metal such that discontinuity stress risers at the interface are inevitable, but its propensity to fracture is more acutely dependent on the externally-induced stress field. It is weak in uniaxial tension and significant in biaxial stress. Therefore, high performance welded shells (biaxial state) will always fail at weld interfaces. It is mildly sensitive to relative material properties of weld and parent materials.

Though weld stresses vary throughout the uniaxial tensile test specimen, the ultimate applied stress should be indicative of the interface uniaxial strength. Also, strains vary along the weld specimen surface [5], slanting stress-strain data to the gage length and location. Therefore, it follows that weld strain data obtained from surface-mounted instrumentation on structural test articles may not be directly correlatable to FEM predictions beyond elastic range.

The peak discontinuity stress occurs on the surface and at weld interfaces. If the peak stress riser in a biaxial field is large, the fatigue life is diminished accordingly. It has no effects on fracture mechanics because its bandwidth is smaller than most detectable flaws.

This concludes responses to the first two questions raised in the introduction.

REFERENCES

1. Structural Strength Program Requirements. MSFC-HDBK-505, Revision A, January 1981.

2. Ryan, Robert S.: Practices in Adequate Structural Design. NASA TP 2893, Marshall Space Flight Center, January 1989, p. 8.

3. McDonough, G.F.: Briefings Related to Qualifying the Solid Rocket Booster Aft Skirt for STS-26, 1988.

4. Berry, David M. and Stansberry, Mark D.: Analysis of Space Shuttle Solid Rocket Booster Aft Skirt Using ANASYS Substructuring, Submodeling, and Plasticity Features. ANSYS 1989 Conference Proceedings, Vol. 1.

5. Vaughn, T.P.: MSFC Metallic Material Division Project 86-020-EH23, Report to be published.

6. ASM Metals Handbook, Ninth edition, Vol. 11, November 1986, p. 434.

7. Flugge, W.: Handbook of Engineering Mechanics. McGraw-Hill Book Company, Part 4, 1962.

APPENDIX A

WELD-PLATE MATERIAL PROPERTIES

The 2219-T87 aluminum structural properties of the plate and forging used in this document were obtained from the MIL-HDBK-C5. Weld properties were developed from 24 specimens excised from an SRB aft skirt which was constructed of 2219 aluminum plate welded to 2219 aluminum forging and heat treated to T87. The TIG weld had a thickness-to-weld ratio of 4.6 as shown in Figure A-1. These specimens were instrumented with electrical strain gages with 0.125-inch length. All specimens were uniaxially stressed in tension to failure in which 21 failed at the forging-weld interface while others failed at the plate interface. Average test results [5] of the weld and the C5 data are plotted in Figure A-2.
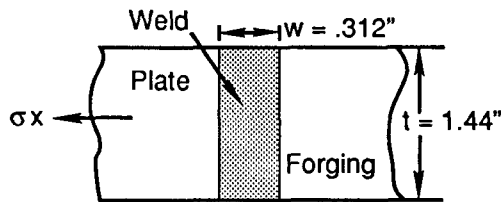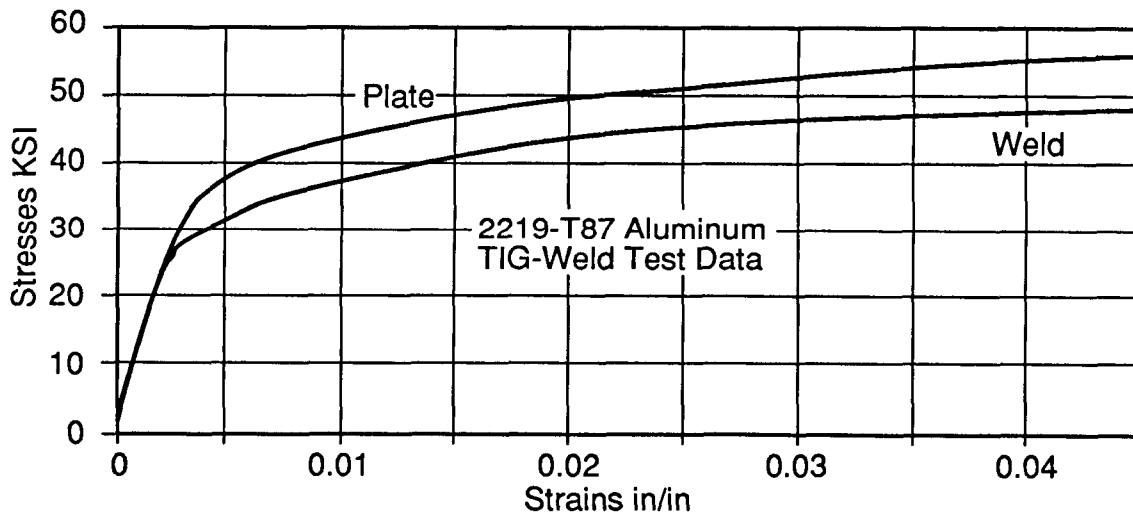
Figure A-1. Weld specimen.

Figure A-2. Uniaxial test specimen properties.

Aluminum stress-strain relationship beyond the elastic limit may be represented by

$$\sigma = a\varepsilon^b \qquad (A\text{-}1)$$

where "a" is the strength coefficient and "b" is the strain-hardening exponent. Both parameters were estimated from Figure A-2 plots and are noted as

	a	b
plate	125	0.24
weld	106	0.23

$\qquad (A\text{-}2)$

Using equation (A-1), the stress-strain variation relationship is calculated from

$$\frac{\Delta\sigma}{\sigma} = abe^{b-1}\,\frac{\Delta\varepsilon}{\varepsilon} \quad ,$$

and letting $\Delta\sigma/\sigma = \delta\sigma$ and $\Delta\varepsilon/\varepsilon = \delta\varepsilon$ gives,

$$\delta\sigma = b\,\delta\varepsilon \qquad (A\text{-}3)$$

It may be reasonable to assume that since strain-hardening alters the stress-strain relationship according to equation (A-1), the same process should adjust the Poisson's ratio between yield and plastic flow. A direct approach is suggested to let the Poisson's ratio vary with the stress beyond the elastic range as

$$\mu = \mu_Y + [\mu_U - \mu_Y]\left[\frac{\sigma - \sigma_Y}{\sigma_U - \sigma_Y}\right] . \qquad (A\text{-}4)$$

where subscripts "U" and "Y" refer to ultimate and yield, respectively. Plate and weld Poisson's ratio were assumed to be,

$$\mu_Y = 0.3 \quad \text{and} \quad \mu_U = 0.5 \ ,$$

and related stresses in ksi are

14

	σ_Y	σ_U
plate	32	58
weld	26	49 .

Respective properties are applied to equation (A-4) to give the following desired relationship:

$$\mu_p = 0.054 + 0.0077\sigma$$

$$\mu_w = 0.074 + 0.0087\sigma \quad .$$

(A-5)

The strain hardening effects on Poisson's ratio may be related to strain by substituting the independent stress variable with equation (A-1). It has the form

$$\mu = C_1 + C_2\, a\varepsilon^b \quad .$$

The secant modulus is used as a relative stiffness parameter,

$$E = \frac{\sigma}{\varepsilon} = \left[\frac{a}{\sigma^{1-b}}\right]^{1/b} \quad .$$

(A-6)

Using plate and weld properties given above, moduli are expressed respectively by

$$E_p = \left[\frac{125}{\sigma^{.76}}\right]^{4.16}$$

(A-7)

$$E_w = \left[\frac{106}{\sigma^{.77}}\right]^{4.34} \quad .$$

Weld data presented is based on strain gages installed on weld surfaces at the center between plate and forging interfaces.

APPENDIX B

DISCONTINUITY STRESS MODEL

The stress problem is defined here as a welded plate which is symmetrical about the midwidth, w/2, and about the midthickness, h. The only external load acting on the weld is an axial tensile stress, σ_x. The weld thickness shrinks at the center as the axial load increases, but it is partially constrained at the plate interface which imposes discontinuity stresses.

The weld interface constraint produces a shear which is zero at the top and bottom surfaces, maximum just below the surfaces, and minimum at the midthickness. This condition may be approximated by adding a dummy piece, as shown in Figure B-1, which allows the weld to be stretched through a dummy unit loading "q" over a length "d." Since this dummy is not part of the weld structure, discontinuity stress distributions for x < d are not relevant to the analysis.
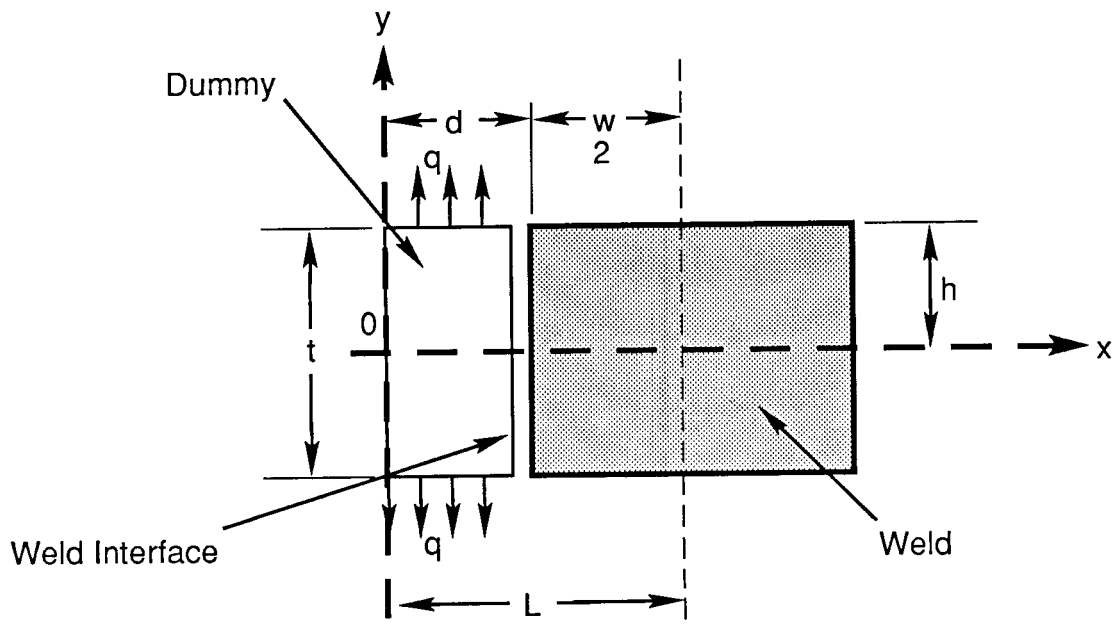

Figure B-1. Weld interface model.

Figure B-1 describes a simply connected contour with in-plane forces which makes it independent of material constants. The geometry and the discontinuous dummy loading "q" is symmetrical about the x and y axes. This is a classical problem [7], applicable to the generalized plane stress method. It consists of integrating the compatibility equation,

$$\frac{\partial^4 \Phi}{\partial x^4} + 2\frac{\partial^4 \Phi}{\partial x^2 y^2} + \frac{\partial^4 \Phi}{\partial y^4} = 0 \quad , \tag{B-1}$$

where Airy's stress function, Φ, is defined by three components derived from equilibrium:

17

$$\sigma_x = \frac{\partial^2 \phi}{\partial y^2} \; ; \quad \sigma_y = \frac{\partial^2 \phi}{\partial x^2} \; ; \quad \tau_{xy} = -\frac{\partial^2 \phi}{\partial x \partial y} \quad . \tag{B-2}$$

Equation (B-1) is of the form $\Phi(x,y) = XY$ whose solution is well known to be

$$\Phi(x,y) = (C_1 \cos \lambda x + C_2 \sin \lambda x)(C_3 \cosh \lambda y + C_4 \sinh \lambda y + C_5 y \cosh \lambda y + C_6 y \sinh \lambda y) \quad , \tag{B-3}$$

where $C_1 \ldots C_6$ are arbitrary constants and $\lambda = m\pi/L$ for $m = 1,2,\ldots$. Substituting equation (B-3) into (B-2), satisfying stress boundary conditions

$$\tau_{xy} = -\frac{\partial^2 \Phi}{\partial x \partial y} = 0 \quad \text{at} \quad x = \pm h \quad \text{and} \quad y = \pm L \quad ,$$

and allowing that $\sin \lambda x$ vanishes for a symmetrical loading of

$$Q = A + \sum_1^n B \cos \frac{\Pi m x}{L} \tag{B-4}$$

at $y = \pm h$, then constants are determined to be

$$C_1 = 1 \quad \text{and} \quad C_2 = C_4 = C_5 = 0 \quad ,$$

and stress components of equation (2) become:

$$\sigma_x = \frac{\partial^2 \phi}{\partial y^2} = 2Q \sum \frac{\cos \lambda x}{2\lambda h + \sinh 2\lambda h} [(\lambda h \cosh \lambda h - \sinh \lambda h) \cosh \lambda y - (\sinh \lambda h) \lambda y \sinh \lambda y]$$

$$\sigma_y = \frac{\partial^2 \phi}{\partial x^2} = 2Q \sum \frac{\cos \lambda x}{2\lambda h + \sinh 2\lambda h} [(\sinh \lambda h) \lambda y \sinh \lambda y - (\lambda h \cosh \lambda h + \sinh \lambda h) \cosh \lambda y]$$

$$\tau_{xy} = -\frac{\partial^2 \Phi}{\partial x \partial y} = 2Q \sum \frac{\sin \lambda x}{2\lambda h + \sinh 2\lambda h} [(\lambda h \cosh \lambda h) \sinh \lambda y - (\sinh \lambda h) \lambda y \cosh \lambda y]. \tag{B-5}$$

Dummy uniform tension loading terms, A and B of equation (B-4), are found in the usual way:

$$\int_{-L}^{L} A \ dx \ = \ \int_{-d}^{d} q \ dx \quad ,$$

or A = qd/L;

$$B \ = \ \frac{2}{L} \int_{-0}^{d} q \ \cos \lambda x \ dx \ + \ \int_{-d}^{L} (0) \ = \ \frac{2q}{\lambda L} \sin \lambda d \quad . \tag{B-6}$$

Evaluating A for integers $0 < m < 1$ in each stress component, A becomes 0 for σ_x and τ_{xy}, and A/2 for σ_y. Assuming that λh is large, then stress discontinuity factors are reduced to:

$$D_y \ = \ \frac{\sigma_y}{q} \ = \ \frac{d}{L} \ + \ 4 \sum \sin \lambda d \ \cos \lambda x \ \frac{e^{-\lambda h}}{\lambda L} \ [(\lambda h + 1) \cosh \lambda y \ - \ \lambda y \ \sinh \lambda y]$$

$$D_x \ = \ \frac{\sigma_x}{q} \ = \ 4 \sum \sin \lambda d \ \cos \lambda x \ \frac{e^{-\lambda h}}{\lambda L} \ [\lambda y \ \sinh \lambda y \ - \ (\lambda h - 1) \ \cosh \lambda y]$$

$$D_{xy} \ = \ \frac{\tau_{xy}}{q} \ = \ 4 \sum \sin \lambda d \ \sin \lambda x \ \frac{e^{-\lambda h}}{\lambda L} \ [\lambda h \ \sinh \lambda y \ - \ \lambda y \ \cosh \lambda y] \quad . \tag{B-7}$$

External loading factor derived from equation (B-4) and discontinuity factors resulting from equation (B-7) are plotted in Figures B-2 and B-3 for $m = \delta$.
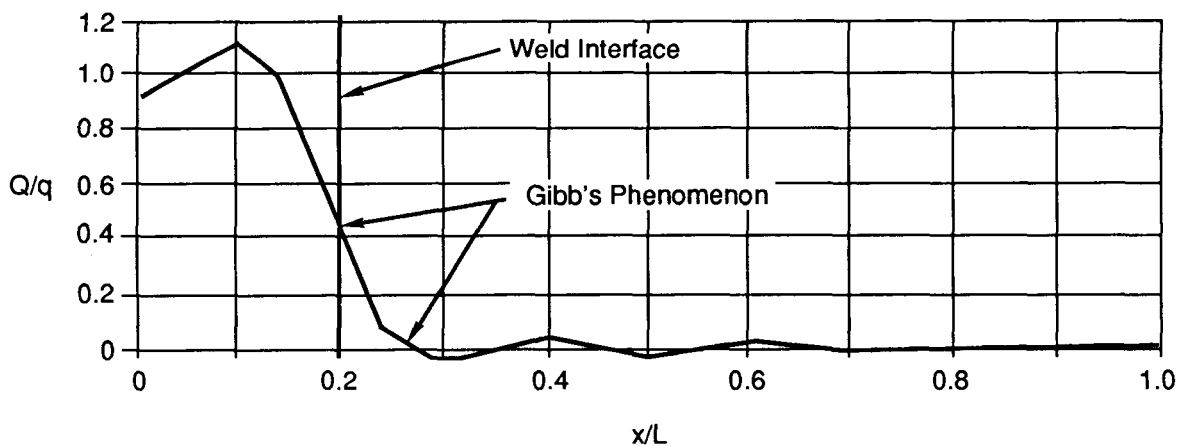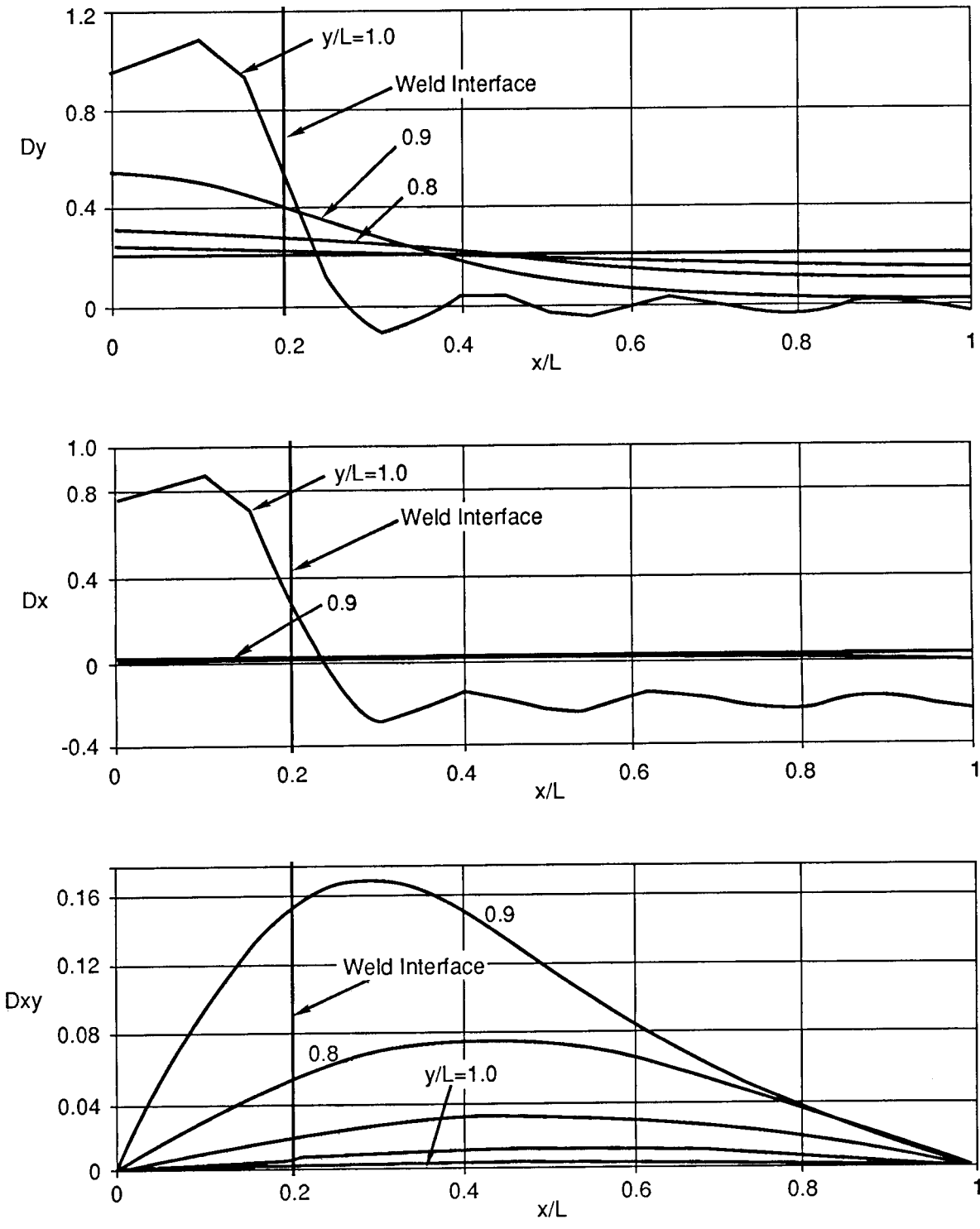

Figure B-2. Dummy loading factor.

Figure B-3. Discontinuity stress component factors.

TECHNICAL REPORT STANDARD TITLE PAGE

1. REPORT NO. NASA TP-2935	2. GOVERNMENT ACCESSION NO.	3. RECIPIENT'S CATALOG NO.
4. TITLE AND SUBTITLE Weld Stresses Beyond Elastic Limit – Materials Discontinuity		5. REPORT DATE August 1989
		6. PERFORMING ORGANIZATION CODE
7. AUTHOR(S) V. Verderaime		8. PERFORMING ORGANIZATION REPORT #
9. PERFORMING ORGANIZATION NAME AND ADDRESS George C. Marshall Space Flight Center Marshall Space Flight Center, Alabama 35812		10. WORK UNIT, NO. M-614
		11. CONTRACT OR GRANT NO.
12. SPONSORING AGENCY NAME AND ADDRESS National Aeronautics and Space Administration Washington, D.C. 20546		13. TYPE OF REPORT & PERIOD COVERED Technical Paper
		14. SPONSORING AGENCY CODE

15. SUPPLEMENTARY NOTES

Prepared by Structures and Dynamics Laboratory, Science and Engineering Directorate.

16. ABSTRACT

When welded structures depend on properties beyond the elastic limit to qualify their ultimate safety factor, and weld-parent materials abruptly change at the interface, then stress discontinuity is inevitable. The stress concentration is mildly sensitive to material relative strain hardening and acutely sensitive to applied stress fields. Peak stresses occur on the weld surface, at the interface, and dissipate within a 0.01-inch band. When the stress is intense, the weld will always fracture at the interface. The analysis incorporates a classical mechanics model to more sharply define stress spikes within the bandwidth, and suggests a relative material index and Poisson's ratio related to strain hardening. Implications are discussed which are applicable to industries of high performance structures.

17. KEY WORDS Weld stress Plastic Interface Discontinuity Fracture	18. DISTRIBUTION STATEMENT Unclassified – Unlimited Subject Category 39

19. SECURITY CLASSIF. (of this report) Unclassified	20. SECURITY CLASSIF. (of this page) Unclassified	21. NO. OF PAGES 32	22. PRICE A03

For sale by National Technical Information Service, Springfield, Virginia 22161

NASA-Langley, 1989